

Tracer diffusion of oxygen in $\text{YBa}_2\text{Cu}_3\text{O}_{7-\delta}$

S. J. Rothman and J. L. Routbort

Materials Science Division, Argonne National Laboratory, Argonne, Illinois 60439

J. E. Baker

Center for Microanalysis of Materials, University of Illinois, Urbana, Illinois 61801

(Received 10 May 1989)

The tracer diffusion of ^{18}O in $\text{YBa}_2\text{Cu}_3\text{O}_{7-\delta}$ has been measured at temperatures from 300 to 850 °C at an oxygen partial pressure of 1×10^5 Pa, and as a function of oxygen partial pressure at 600 °C. The diffusion of oxygen is strongly anisotropic. The faster component, associated with diffusion in the ab plane, has an activation energy of 0.97 ± 0.03 eV. There is no break in the Arrhenius plot at the orthorhombic-tetragonal transformation temperature. The diffusion coefficient is not a strong function of oxygen partial pressure from 3×10^3 to 1×10^5 Pa at 600 °C. The results are compared to the predictions of the various theories of diffusion in $\text{YBa}_2\text{Cu}_3\text{O}_{7-\delta}$.

I. INTRODUCTION

The critical superconducting transition temperature T_c in cupric oxide perovskite-structure superconductors is a sensitive function of the deviation from stoichiometry. In $\text{YBa}_2\text{Cu}_3\text{O}_{7-\delta}$, T_c is a maximum for $\delta=0$ and is 0 for $\delta \approx 0.5$.¹ Since the nonstoichiometry is due to oxygen ion vacancies, it is important to study and understand their behavior in these materials. Tracer diffusion measurements are an established technique for investigating the behavior of vacancies in solids. Oxygen tracer diffusion measurements in $\text{YBa}_2\text{Cu}_3\text{O}_{7-\delta}$ also have an intrinsic interest because of the additional complexities of these systems, namely, the anisotropy of the structure, the ordering of the vacancies at low temperature, and the large concentration of vacancies which can be obtained on the oxygen sublattice.

The fraction of vacant oxygen ion sites δ is a function of temperature and oxygen partial pressure. Neutron diffraction studies² of the structure of $\text{YBa}_2\text{Cu}_3\text{O}_{7-\delta}$ (Fig. 1) have shown that at low temperatures (< 300 °C) and high P_{O_2} ($\approx 10^5$ Pa), δ is close to 0 (≈ 0.05), the O(1) sites are filled with oxygen ions, and the O(5) sites are empty, i.e., the vacancies and oxygen ions on these planes are ordered. When the material is heated at constant P_{O_2} , δ increases and the mobile oxygen ions on the O(1) sites (the "chains" in the ab plane) begin to disorder, some of them moving onto O(5) sites, and some leaving the material, until at the temperature of the orthorhombic-tetragonal ($O-T$) phase transformation (≈ 680 °C at $P_{\text{O}_2} = 10^5$ Pa), $\delta=0.5$ and the oxygen ions are evenly distributed over O(1) and O(5) sites. There is a strong implication in the neutron diffraction results that diffusion in the c direction in this structure is very slow, as there is no easy path for an oxygen ion vacancy to move from one ab plane to a neighboring one

The unusual structure and behavior of $\text{YBa}_2\text{Cu}_3\text{O}_{7-\delta}$ has led to a number of theoretical attempts to elucidate the diffusion behavior of the oxygen ions. The ordered

state of the vacancies and oxygen ions in $\text{YBa}_2\text{Cu}_3\text{O}_{7-\delta}$ suggested to Ronay and Nordlander³ that oxygen could move interstitially along the channels parallel to the b axis. Their calculations showed that the activation energy for such motion would be near zero, which implies very fast diffusion along the b axis compared to the other two principal axes. For the latter they calculated an activation energy for motion of ≈ 1.6 eV.

The details of the atomic jumps in the ab plane have been considered by Tu *et al.*⁴ and Bakker *et al.*,⁵ both of these groups considered $D_c \approx 0$, where D_c is the tracer diffusion coefficient along the c direction. The former considered that the force between two neighboring oxygens ions was repulsive for an O(1) and an O(5) site, repulsive for two O(1) sites in the a direction and attrac-

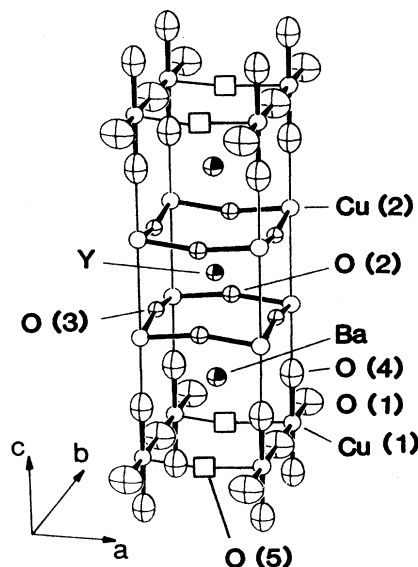


FIG. 1. Structure of $\text{YBa}_2\text{Cu}_3\text{O}_{7-\delta}$. From Ref. 2.

tive in the b direction. The activation energy that resulted from the calculation was greater in the a than in the b direction, and therefore $D_b > D_a$. The calculated activation energy for diffusion in the b direction was 1.3 eV for $\delta=0$. A much lower activation energy, about 0.5 eV, was estimated for diffusion in material with $\delta=0.38$. Correlation effects were neglected in this calculation.

Bakker *et al.*⁵ calculated the interaction energies between vacancies from the thermodynamic parameters derived from the temperature dependence of the oxygen site occupation. They showed that the tracer diffusion coefficient has the usual form

$$D = \frac{1}{2} p_v \omega f d^2 \quad (1)$$

for diffusion in the ab plane, where p_v is the vacancy availability factor (the probability that a vacancy is next to a given atom), ω is the exchange frequency between the atom and the neighboring vacancy, f is the Bardeen-Herring correlation factor for oxygen diffusion, and d is the jump distance. The O(1) and the O(5) sites were considered to be on a square lattice in this treatment, and the slight anisotropy of the lattice parameter in the ab plane was neglected. The basic jump was the O(1)-O(5) or the O(5)-O(1). Since at least half of the total number of these sites is empty, $p_v \approx 1$ at all temperatures and consequently D would have a weak dependence on oxygen partial pressure P_{O_2} .

In this model, ω was assumed to have an Arrhenius dependence. The activation energy was obtained by normalization to experimental data because the configuration of the saddle point was not precisely known. The physics of the diffusion was contained mostly in the correlation factor f , which measures the probability that an ion will not return to its original site immediately after completing a jump. The value of f is low (≈ 0.1) at low temperatures and small δ when the oxygen ions and vacancies are ordered, but increases to $f \approx 1$ at high temperatures where the disorder on the O(1) and the O(5) sites is almost complete.

Our preliminary measurements of D for ^{18}O in $\text{YBa}_2\text{Cu}_3\text{O}_{7-\delta}$ have been reported in the proceedings of various conferences.⁶⁻⁹ The data in Refs. 6-8 were limited to $\text{YBa}_2\text{Cu}_3\text{O}_{7-\delta}$ from one batch of material, a narrow temperature range ($300 \leq T \leq 600^\circ\text{C}$) and one value of P_{O_2} , 1×10^5 Pa. This paper reports an investigation on two batches of $\text{YBa}_2\text{Cu}_3\text{O}_{7-\delta}$, extension of the temperature range across the O - T transformation to 850°C , and variation of the P_{O_2} by a factor of 30 at 600°C . The results are compared to the predictions of the three theories outlined above.

II. EXPERIMENTAL

A. Sample preparation

One batch of powders (material No. 1) was prepared by milling together reagent grade Y_2O_3 , BaCO_3 , and CuO , pressing, and calcining at 890°C . The pellets were crushed, pressed, and fired twice before the final grinding. The resulting powders, $2.5 \mu\text{m}$ in size, were pressed at 15

MPa and fired in pure O_2 according to the following schedule: $5^\circ\text{C}/\text{min}$ to 965°C , $1^\circ\text{C}/\text{min}$ to 985°C , 120 min hold, furnace cool. This material showed some preferred orientation with the c axis parallel to the pressing direction. The material was phase-pure as determined from x-ray diffraction. The density of the pellets was $\approx 99\%$ of theoretical. A micrograph of this material taken with polarized light (Fig. 2) exhibited the familiar elongated grains with aspect ratios ranging from 10 to 100. Heat treatment in O_2 for 12 h at 400°C produced a superconductor with $T_c \approx 90\text{K}$. This material was stoichiometric, and contained ≈ 1300 ppm by wt. Sr and ≈ 1000 ppm Zr as major impurities, as well as ≈ 70 ppm Ca and traces of Ni, Cr, and Mn.

Another batch of material (material No. 2) was prepared from powder obtained from Rhone-Poulenc, Inc. The powder, $1.4 \mu\text{m}$ in size, contained about 90 ppm Ti, 75 ppm Fe and 200 ppm Ca+Sr (by weight) as the principal cation impurities. The samples were pressed at 70 MPa, sintered in pure O_2 at 975°C for 4 h, cooled to 530°C at a rate of about $5^\circ\text{C}/\text{min}$, and then cooled to 400°C over a span of 15 h, following which the furnace was cooled to room temperature in about 3 h. T_c was approximately 90 K and the critical current density at 77 K was only $50 \text{ A}/\text{cm}^2$. The microstructure of material No. 2 was similar to that of material No. 1, but the grains were somewhat larger. Material No. 2 contained 3-4 at. % excess Cu.

Samples were polished down to $1\text{-}\mu\text{m}$ diamond paste. In order to avoid degradation due to moisture, no aqueous solutions were used in polishing or cleaning, and samples were stored in a desiccator.

The object of these experiments was to measure the tracer and not the chemical diffusion coefficient. Since oxygen has no useful radioactive isotope, the stable isotope ^{18}O (natural background: 0.204%) was used as the tracer. The stoichiometries of the samples were adjusted prior to the diffusion anneals in order to avoid any gradient of the chemical potential of oxygen during the diffusion anneal in ^{18}O . Samples were given a prediffusion anneal at the same temperature and P_{O_2} as



FIG. 2. Micrograph of $\text{YBa}_2\text{Cu}_3\text{O}_{7-\delta}$ made from material No. 1 taken using polarized light. The bar represents $100 \mu\text{m}$.

were planned for the diffusion anneal, but for a much longer time than the diffusion annealing time, and under ^{16}O instead of ^{18}O . Thus, even though the entire sample may not have been equilibrated at T and P_{O_2} , a shell much thicker than the diffusion penetration was, equilibrated. This minimized the chemical potential gradient in the diffusion zone.

Initial experiments indicated that the exchange of oxygen was hindered by a surface reaction, especially at low temperatures. Therefore, the polished and preannealed samples were implanted with $\approx 10^{17}$ ions/cm 2 ^{18}O at 5 keV. The mean range of these ions was only ≈ 100 Å and the amount implanted made only a small contribution to the indiffused ^{18}O . The implanted samples were annealed in quartz capsules, which had been backfilled with 95% ^{18}O to the same P_{O_2} and sealed off. The annealing temperature was measured to ± 1 °C.

B. Depth profiling technique

Since ^{18}O is not radioactive, secondary ion mass spectrometry (SIMS) was used as the depth-profiling technique. The SIMS technique has been successfully employed for measurements of oxygen diffusion in a wide-variety of ceramic oxides $^{10-13}$ and its application to the study of oxygen diffusion in the 37-K superconductor $\text{La}_{2-x}\text{Sr}_x\text{CuO}_4$ has been recently described. 14

Concentration profiles were measured on the Cameca 3f SIMS at the Center for the Microanalysis of Materials at the University of Illinois, Urbana. A beam of 17-eV Cs^+ ions was used to sputter the surface and the secondary ions were mass spectrographically analyzed. The operating conditions were primary beam current $\approx 0.2-0.3$ μA , beam diameter ≈ 60 μm , raster 250×250 μm^2 , analyzed area 10- μm in diameter, and masses of 16, 18, and 63 counted by negative SIMS for 1 s each. Crater depths were measured with a profilometer. The depth corresponding to each channel was assumed to be the total crater depth divided by the number of channels. This mode of determining the concentration as a function of distance is referred to as a spot scan; because of time limitations and roughening of the crater bottoms, this method was not used for diffusion zones deeper than ≈ 10 μm . A typical depth profile from a spot scan is shown in Fig. 3.

When the diffusion zone was much deeper than 10 μm , a taper section (1–2°) was ground on the sample after the diffusion anneal. The angle of the taper was measured with a profilometer. The penetration profile was measured by automatically stepping an unrastrered beam in 25- or 50- μm steps along the taper. This mode is referred to as a line scan, and a typical one is shown in Fig. 4. In some cases, manual stepping was used in order to avoid cracks. The depth corresponding to each channel was taken as the distance along the taper times the sine of the taper angle. In both modes the concentration c of tracer for each channel was determined by subtracting the ^{18}O background from the ^{18}O counts and dividing by the sum of ^{16}O and ^{18}O counts.

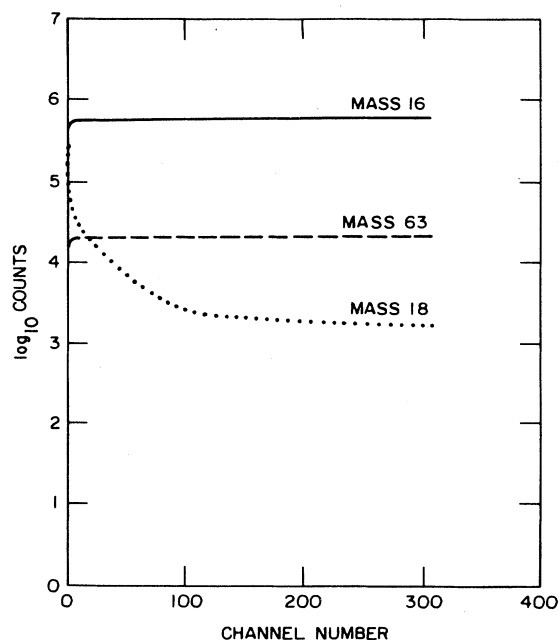


FIG. 3. Typical spot scan, showing the logarithm of counts of ^{16}O , ^{18}O , and ^{63}Cu as a function of channel number (proportional to penetration distance).

III. RESULTS

The analysis of a depth profile to obtain a value of D must begin with considering how the SIMS beam averaged over the different grain orientations in the specimen. The analyzed area was always 10- μm in diameter. According to Fig. 2, an area of this size would include parts of several grains, unless a lucky hit were scored on a single large grain. In the spot-scan mode, described above, the same set of grains would probably be analyzed over the entire depth profile. On the other hand, each 25- or 50- μm step in a line scan would move the analyzed area

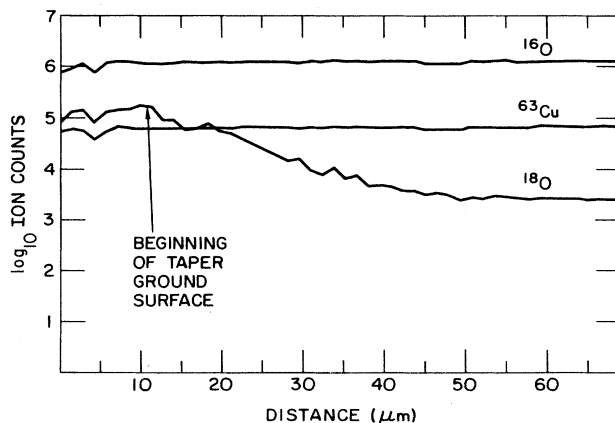


FIG. 4. Typical line scan, showing the logarithm of counts of ^{16}O , ^{18}O , and ^{63}Cu vs depth; the depth equals the distance along the taper section times the sine of the taper angle.

to a different set of grains. The two different methods of obtaining depth profiles can thus be expected to lead to different analyses.

The penetration plots obtained from the spot scan method can be expected to be the sum of the depth profiles of the individual grains, each with a multiplier proportional to the cross-sectional area of that grain, and each with a value of D corresponding to the orientation of that grain with respect to the diffusion direction. These values of D may differ considerably because of the anisotropy of diffusion in the $\text{YBa}_2\text{Cu}_3\text{O}_{7-\delta}$ lattice. Such a penetration plot would therefore be fitted to an equation of the form

$$c = A_1 \operatorname{erfc} \left[\frac{x}{2(D_1 t)^{1/2}} \right] + A_2 \operatorname{erfc} \left[\frac{x}{2(D_2 t)^{1/2}} \right], \quad (2)$$

where c is the concentration at depth x and t is the diffusion time. In principle, Eq. (2) should contain a term for each grain in the analysis area, but the number of terms has been limited to two in order to keep the number of parameters within reason. The erfc solution corresponds to the boundary condition of constant concentration at the surface.

On the other hand, in a line scan, the concentration at each point represents the concentration in a different group of grains, so the depth profile would be represented by

$$c = A \operatorname{erfc} \left[\frac{x}{2(Dt)^{1/2}} \right], \quad (3)$$

but D would be averaged (in the manner indicated above) over all the grains hit in the line scan. The anisotropy of diffusion is indicated in this type of scan by fluctuations in the ^{18}O count observed in the diffusion zone of the line scan of Fig. 4. Fluctuations only occur in the ^{18}O counts at concentrations above background; they do not occur in the ^{16}O or ^{63}Cu counts. This suggests that these fluctuations are not noise. Since each point represents a different group of grains, scatter due to anisotropy would not be surprising.

In the preliminary analyses of the data on material No. 2,⁶⁻⁸ the fast diffusion term was thought to represent diffusion along a short-circuiting path, and so the form of this term was chosen as the usual grain boundary diffusion expression, $A_1 \exp[-(Zx)^{6/5}]$, where A_1 is the multiplier and Z contains the grain boundary diffusion coefficient. The analysis in terms of contributions from the volume of two different grains is preferred because the multipliers for the fast and slow diffusion terms are the same order of magnitude, whereas if the fast diffusion term represented diffusion along a short-circuiting path, the multiplier for this term should be much smaller than for the slow (volume) diffusion term, as was indeed the case in $\text{La}_{2-x}\text{Sr}_x\text{CuO}_4$.¹⁴ There is little difference between the goodness of these two types of fit, as measured by χ^2 and the randomness of the deviations of the experimental data around the least-squares line.

A penetration plot obtained from a spot scan of $\text{YBa}_2\text{Cu}_3\text{O}_{7-\delta}$ (material No. 2) annealed for $\frac{1}{2}$ h at 300°C

with $P_{\text{O}_2} = 10^5$ Pa is shown in Fig. 5. The experimental points are shown as circles, while the solution to the diffusion equation, Eq. (2), is shown as a solid line. A penetration plot obtained from a line scan is shown in Fig. 6 for a sample of material No. 1 annealed for $\frac{1}{3}$ h at 850°C with $P_{\text{O}_2} = 10^5$ Pa; here the line is the fit to Eq. (3).

Both types of fits were carried out by a nonlinear least-squares routine.¹⁵ The values of D obtained by the two techniques agree well (Table II). The same values of D were also obtained in directions parallel or transverse (denoted by TS in the table) to the pressing direction on the textured specimens (material No. 1).

The following experimental uncertainties enter into the use of SIMS to measure diffusion coefficients. The standard deviations about the fits are, for the most part, only a few percent. Uncertainties in the crater depths caused by surface roughness, for example, or in the position and taper angle for line scans, could lead to an uncertainty of 20% in D . However, the scatter from duplicate samples is larger than this. The standard error for diffusion measurements on oxides using SIMS seems to be about a factor of 2.¹³ We believe, therefore, that the scatter above this level observed at, for example, 400°C , is probably due to anisotropy.

The diffusion coefficients for the fast-diffusing component (D_1) and the diffusion coefficients obtained from line scans in material #1 at $P_{\text{O}_2} = 10^5$ Pa are plotted together in the usual Arrhenius form in Fig. 7; data for longitudinal and transverse samples have been given different symbols. A fit to these data yields

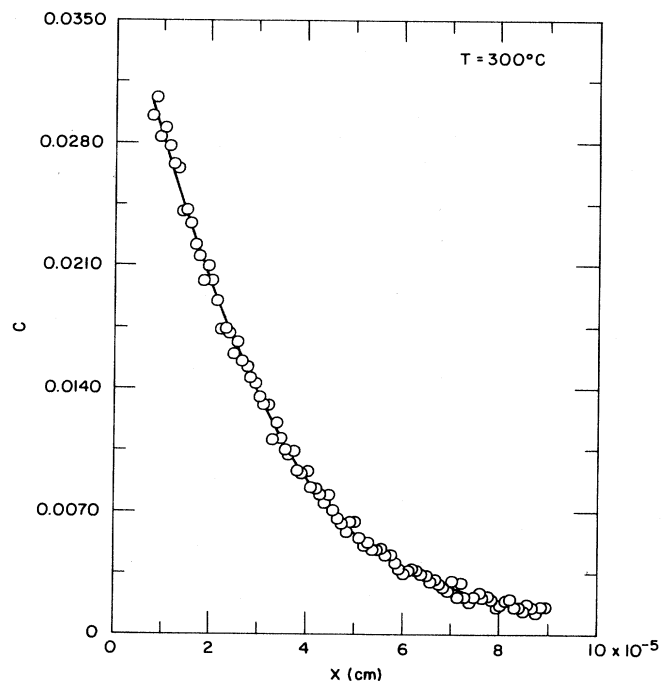


FIG. 5. Penetration plot from a spot scan for $\text{YBa}_2\text{Cu}_3\text{O}_{7-\delta}$ (material No. 2) annealed for $\frac{1}{2}$ h at 300°C at $P_{\text{O}_2} = 10^5$ Pa. The solid line is the nonlinear least-squares regression fit to Eq. (2).

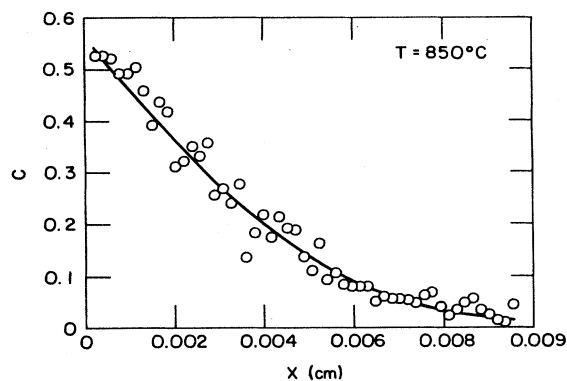


FIG. 6. Penetration plot from a line scan on a taper section for $\text{YBa}_2\text{Cu}_3\text{O}_{7-\delta}$ (material No. 1), annealed for $\frac{1}{3}$ h at 850°C at $P_{\text{O}_2} = 10^5$ Pa. The solid line is the nonlinear least-squares regression fit to Eq. (3).

$D_1 = [(1.4 \pm 0.6) \times 10^{-4}] \exp[-(0.97 \pm 0.03 \text{ eV}/kT)]$ (4)
in cm^2s^{-1} . These parameters differ only slightly from the ones obtained if only the largest D_1 at each temperature is used; the latter are most likely to correspond to diffusion in the same crystal direction.

The data for D_1 obtained from material No. 2 have been plotted in Fig. 8. The fit yields

$$D_1 = [(1.3 \pm 1.5) \times 10^{-6}] \times \exp[-(0.68 \pm 0.08 \text{ eV}/kT)] \text{ cm}^2\text{s}^{-1}. \quad (5)$$

The parameters given in the Arrhenius equation for material #2 differ from those previously published for this

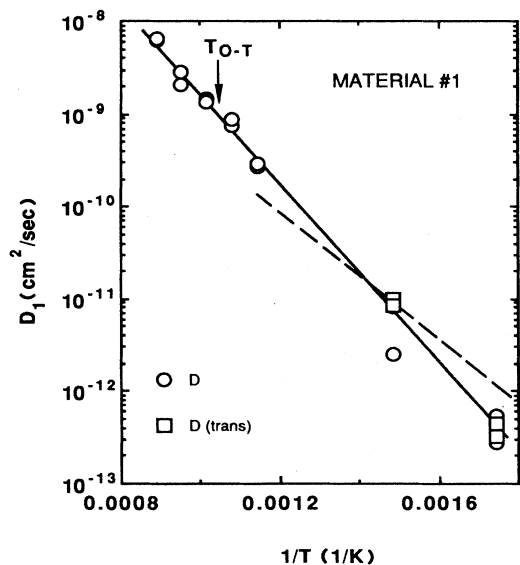


FIG. 7. Arrhenius plot of the fast-diffusing component D_1 , measured for material No. 1 for $P_{\text{O}_2} = 10^5$ Pa. The solid line is the least-squares fit to the data. The dashed line is the fit to the data for material No. 2.

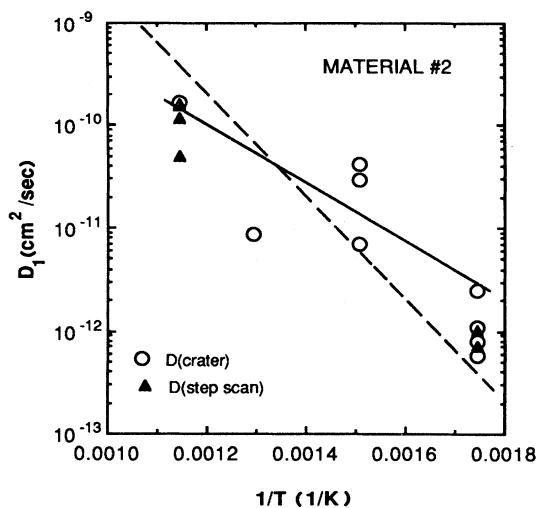


FIG. 8. Arrhenius plot of the fast-diffusing component D_1 , measured for material No. 2 at $P_{\text{O}_2} = 10^5$ Pa. The solid line is the least-squares fit to the data. The dashed line is the fit to the data for material No. 1.

material⁶⁻⁸ because, as just mentioned, the functional fit of the data was changed from a complementary error function with a grain boundary tail to the sum of two complementary error functions.

The data for the slow-diffusing component D_2 measured in both materials are presented in Fig. 9. The scatter from material to material and within each material is very large probably because of material differences and anisotropy. No attempt was made to fit these data.

The variation of the oxygen diffusion coefficient in material #1 at 600°C with P_{O_2} from 3×10^3 to 10^5 Pa (Fig.

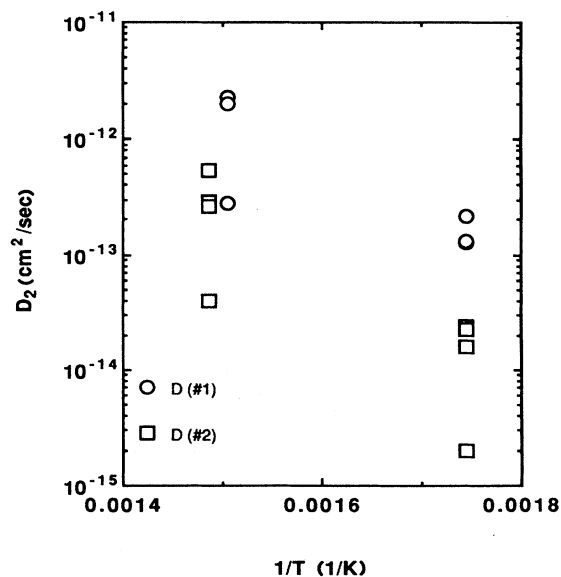


FIG. 9. Arrhenius plot of the slow-diffusing component D_2 , measured for both materials at $P_{\text{O}_2} = 10^5$ Pa.

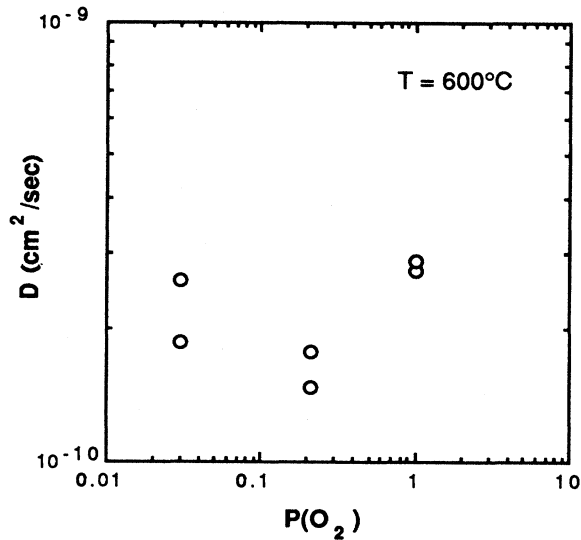


FIG. 10. Dependence of D_1 on $\text{Log } P_{\text{O}_2}$ for material No. 1 at 600°C .

10) may or may not be within the experimental uncertainty; clearly there is no strong dependence on the oxygen partial pressure.

IV. DISCUSSION

Four main topics will be discussed: anisotropy of diffusion, comparison of the results obtained for materials

No. 1 and No. 2, a comparison of these results with those reported by other workers, and finally, a comparison to the theories introduced in Sec. I.

A. Anisotropy

The diffusion coefficient for an arbitrary direction in an orthorhombic crystal is given by¹⁶

$$D = D_a \cos^2\Theta_a + D_b \cos^2\Theta_b + D_c \cos^2\Theta_c, \quad (6)$$

where the coefficients are the diffusion coefficients in the three principal crystal directions and the $\cos\Theta$ are the direction cosines of the arbitrary direction with respect to the three principal axes.

Initial results for oxygen diffusion in the c direction in a $\text{YBa}_2\text{Cu}_3\text{O}_{7-\delta}$ single crystal at 430°C indicate that D_c is approximately three orders of magnitude smaller than D for the polycrystals.¹⁷ However, the present experimental conditions are such that the contribution from a D this small would not be observed, for the following reason. Because the values of D in the polycrystalline samples are much greater, the annealing times used were relatively short ($\leq \frac{1}{2}$ h), so diffusion parallel to the c axis would result in a narrow ($\approx 100 \text{ \AA}$) peak near the surface. In a spot scan, this peak would be inseparable from the near-surface noise and the remnant of the implanted ^{18}O , and it would also be missed in a line scan because the first step is not exactly at the surface. Furthermore, if the slow component were close to the c direction, the D_1/D_2 ratio would have to be about 10^3 .

TABLE I. Diffusion coefficients for material No. 1. $P_{\text{O}_2} = 10^5$ Pa unless noted otherwise.

T ($^\circ\text{C}$)	Sample number ^a	D_1 (cm^2/s)	D_2 (cm^2/s)	Comments ^b
300	1	$(2.77 \pm 0.17) \times 10^{-13}$	$(1.59 \pm 0.12) \times 10^{-14}$	SS
300	1	$(5.40 \pm 0.79) \times 10^{-13}$	$(2.42 \pm 0.52) \times 10^{-14}$	SS
300	2	$(4.38 \pm 0.36) \times 10^{-13}$	$(2.26 \pm 0.62) \times 10^{-14}$	SS,TS
300	2	$(3.27 \pm 0.20) \times 10^{-13}$	$(1.98 \pm 0.30) \times 10^{-15}$	SS,TS
400	3	$(2.50 \pm 0.04) \times 10^{-12}$	$(3.90 \pm 0.60) \times 10^{-14}$	SS
400	3	$(8.22 \pm 0.17) \times 10^{-12}$	$(2.89 \pm 0.16) \times 10^{-13}$	SS
400	4	$(1.01 \pm 0.05) \times 10^{-11}$	$(5.31 \pm 0.66) \times 10^{-13}$	SS,TS
400	4	$(8.59 \pm 0.23) \times 10^{-12}$	$(2.64 \pm 0.52) \times 10^{-13}$	SS,TS
600	5	$(2.72 \pm 1.00) \times 10^{-10}$		LS
600	5	$(2.87 \pm 1.06) \times 10^{-10}$		LS
652	6	$(8.60 \pm 0.66) \times 10^{-10}$		LS
652	6	$(7.39 \pm 0.52) \times 10^{-10}$		LS
711	7	$(1.43 \pm 0.13) \times 10^{-9}$		LS
711	7	$(1.33 \pm 0.11) \times 10^{-9}$		LS
780	8	$(2.09 \pm 0.10) \times 10^{-9}$		LS
780	8	$(2.89 \pm 0.15) \times 10^{-9}$		LS
850	9	$(6.47 \pm 0.23) \times 10^{-9}$		LS
850	9	$(6.18 \pm 0.27) \times 10^{-9}$		LS
600	10	$(1.86 \pm 0.50) \times 10^{-10}$		LS, $P_{\text{O}_2} = 3 \times 10^3$ Pa
600	10	$(2.59 \pm 0.62) \times 10^{-10}$		LS, $P_{\text{O}_2} = 3 \times 10^3$ Pa
600	11	$(1.76 \pm 0.53) \times 10^{-10}$		LS, $P_{\text{O}_2} = 2 \times 10^4$ Pa
600	11	$(1.47 \pm 0.24) \times 10^{-10}$		LS, $P_{\text{O}_2} = 2 \times 10^4$ Pa

^aShown to indicate that some data were taken with multiple craters or scans.

^bSS = spot scan, LS = line scan, TS = transverse section.

TABLE II. Diffusion coefficients for material No. 2 at $P_{O_2} = 10^5$ Pa.

$T(^{\circ}\text{C})$	Sample Number ^a	D_1 (cm ² /s)	D_2 (cm ² /s)	Comments ^b
300	1	$(5.66 \pm 0.38) \times 10^{-13}$	$(1.26 \pm 0.08) \times 10^{-13}$	SS
300	1	$(2.45 \pm 0.16) \times 10^{-12}$	$(2.14 \pm 0.04) \times 10^{-13}$	SS
300	2	$(7.94 \pm 0.92) \times 10^{-13}$	$(1.31 \pm 0.07) \times 10^{-13}$	SS
300	2	$(1.11 \pm 0.02) \times 10^{-12}$	$(2.15 \pm 0.18) \times 10^{-13}$	SS
300	3	$(1.03 \pm 0.09) \times 10^{-12}$		LS
300	3	$(7.14 \pm 1.73) \times 10^{-13}$		LS
391	4	$(4.19 \pm 0.63) \times 10^{-11}$	$(2.02 \pm 0.02) \times 10^{-12}$	SS
391	4	$(6.97 \pm 0.13) \times 10^{-12}$	$(2.76 \pm 0.18) \times 10^{-13}$	SS
391	5	$(2.95 \pm 0.10) \times 10^{-11}$	$(2.27 \pm 0.40) \times 10^{-12}$	SS
600	6	$(1.67 \pm 0.02) \times 10^{-10}$		SS
600	7	$(1.54 \pm 0.11) \times 10^{-10}$		LS
600	7	$(1.60 \pm 0.10) \times 10^{-10}$		LS
600	7	$(4.96 \pm 0.42) \times 10^{-11}$		LS
600	7	$(1.16 \pm 0.08) \times 10^{-10}$		LS

^aShown to indicate that some data were taken with multiple craters or scans.

^bSS=spot scan, LS=line scan

Inspection of Tables I and II indicates that $D_1/D_2 \ll 10^3$. Therefore, one may conclude that the slow contribution D_2 does not correspond to diffusion along the c axis, but represents diffusion in the ab plane of a grain oriented so that the ab plane makes a bigger angle with the diffusion direction than the ab plane of the grain from which D_1 was obtained. From our data it is not possible to draw any conclusions concerning anisotropy in the ab plane; because of the heavily twinned structure of the orthorhombic material, even measurements on single crystals may not resolve this question.

The anisotropy observed in $\text{YBa}_2\text{Cu}_3\text{O}_{7-\delta}$ is in accord with the neutron diffraction result that the mobile oxygen ions occupy the O(1) sites² and with the perception that the distance between oxygen sites along the c axis is too long for a jump to take place easily (Fig. 1). This behavior contrasts with the observation that in $\text{La}_{2-x}\text{Sr}_x\text{CuO}_4$, one volume component and a short-circuiting component is sufficient to fit the depth profiles, even though the oxygen ion vacancies are located on one type of sites in the ab plane in $\text{La}_{2-x}\text{Sr}_x\text{CuO}_4$,¹⁸ just as they are in $\text{YBa}_2\text{Cu}_3\text{O}_{7-\delta}$.

B. Comparison of materials

A glance at Figs. 7 and 8 indicates that D_1 for material No. 1 was lower than for material No. 2 at 300°C, but higher at 600°C. The data from material No. 2 exhibit considerably more scatter than do the data from material No. 1. The slow component D_2 was smaller for material No. 1 than for material No. 2 over the temperature range 300–400°C. Both materials had a wide distribution of grain sizes, but on the average, material No. 1 had the smaller grain size. Samples containing larger grains would tend to exhibit more scatter because the SIMS beam would sample fewer orientations. Materials No. 1 and No. 2 also differed in that the latter contained 3–4

at. % excess Cu, and the sintering behavior of the two materials was quite different.¹⁹ It is unlikely that the impurity concentration, which is much smaller than the concentration of oxygen ion vacancies, influences the value of D .

C. Comparison with other results

The tracer diffusion of oxygen in $\text{YBa}_2\text{Cu}_3\text{O}_{7-\delta}$ has been measured²⁰ by following the exchange of ^{18}O in the atmosphere with ^{16}O in $\text{YBa}_2\text{Cu}_3\text{O}_{7-\delta}$ powders *in situ* with a microbalance. The results in the temperature range of ≈ 250 to 420°C at $P_{O_2} = 6.5 \times 10^3$ Pa ($\delta \approx 0.07$) were

$$D = 0.287 \exp[-(1.7 \text{ eV}/kT)]$$

cm² s⁻¹. However, the exchange of oxygen between the gas and the powder was, according to the authors, limited by a surface reaction at low temperature; we do not believe that a diffusion coefficient can be obtained from an integral measurement under this condition. The diffusion coefficients are considerably lower by (10^3 at 350°C) than those reported here and the activation energy is nearly a factor of 2 higher than our value of 0.97 eV; it is exactly equal to the one observed by Tu *et al.*⁴ for out diffusion limited by surface reaction. Furthermore, whereas we observe a small increase (≈ 2) in D with increasing P_{O_2} at 600°C in the orthorhombic phase ($P_{O_2} > 10^4$ Pa, Fig. 10), Ikuma and Akiyoshi²⁰ reported a large decrease of D with increasing δ for $T > 420^\circ\text{C}$, corresponding to a decrease in D with a decrease in P_{O_2} . Therefore their results are in disagreement with the results of our experiments in all aspects; however, as indicated above, we do not believe that their low-temperature results represent diffusion.

Tallon and Staines²¹ observed a relaxation peak in the internal friction of $\text{YBa}_2\text{Cu}_3\text{O}_{7-\delta}$ at 40 kHz at ≈ 800 K, which they ascribed to oxygen hopping. They calculated

an oxygen tracer diffusivity by assuming that the peak had a Debye shape and by using a simple model of the diffusive jump (no correlation). They obtained an activation energy of about 1 eV for $T < 500^\circ\text{C}$. Above this temperature, their Arrhenius plot curved sharply upwards.

Although the absolute values of D calculated from the internal friction agree reasonably well with the values of D_1 measured for material No. 1, their results disagree with ours in other ways. First, within the accuracy of our measurements, we obtain no curvature in the Arrhenius plot. Second, Tallon and Staines find that D decreases with increasing P_{O_2} in both the orthorhombic and tetragonal phases (by, for example, a factor of ≈ 7 from 8×10^4 to 2×10^3 Pa at 600°C), in contradiction to our observation of no strong pressure dependence (within a factor of 2) of D in this pressure range. Certainly one possible source of a disagreement can be in the microstructure and in the chemistry of the samples. Other principal concerns about the results of Tallon and Staines are the neglect of the correlation factor, which is expected to be a function of temperature,^{5,22} and the assumption of a Debye peak shape.

Most investigations of oxygen diffusion in $\text{YBa}_2\text{Cu}_3\text{O}_{7-\delta}$ have been carried out under a gradient of oxygen chemical potential and have therefore measured a chemical diffusion coefficient,²³ \bar{D} , given by

$$\bar{D} = \frac{1}{2} d^2 \omega f_v (1 + \partial \ln \gamma / \partial \ln c) . \quad (7)$$

The chemical diffusion coefficient differs from the tracer diffusion coefficient Eq. (1) in that (1) the correlation factor contained in Eq. (7), f_v is the correlation factor for the diffusion of vacancies, and not a tracer correlation factor;²⁴ (2) \bar{D} does not contain the vacancy availability factor, since chemical diffusion deals with the diffusion of the defects, vacancies in this case; and (3) \bar{D} does contain the thermodynamic factor²⁵ (the term in parentheses above; γ is the oxygen activity coefficient), which takes account of the fact that the driving force in a chemical diffusion experiment is the gradient in the *chemical potential*, and not in the concentration. The first two of these probably do not cause the tracer and chemical diffusion coefficients to differ since f_v is probably close to the correlation factor for tracer diffusion, and the vacancy availability factor is close to unity in the framework of the model of Bakker *et al.*²² However, the value of the thermodynamic factor may differ greatly from unity, and may depend strongly on temperature in a highly nonideal substance like $\text{YBa}_2\text{Cu}_3\text{O}_7$.²² The chemical and tracer diffusion coefficients can differ considerably because of the thermodynamic factor.

Another difference between \bar{D} and D lies in the method of measurement. The present tracer diffusion coefficients were obtained by a depth profiling technique, in which the distances were determined with some precision. The chemical diffusion coefficient is usually measured by changing P_{O_2} around a sample, and following the relaxation of some physical property (weight, electrical resistivity) as the sample picks up or loses oxygen. The result of such a measurement is a relaxation time, and the dis-

tance over which the diffusion takes place must also be measured or modeled in order to obtain a diffusion coefficient. In the case of cracked or porous samples, such a measurement may not be accurate, and an incorrect measurement can lead to a diffusion coefficient that is high by orders of magnitude. We believe that the scatter of the values of the chemical diffusion coefficient, noted in our survey of the literature in Ref. 9, is due to sample quality, especially porosity or microcracking. In general, the values of \bar{D} are greater than the values of D .

A value of 1.51 eV has been obtained for the activation energy for oxygen diffusion in $\text{YBa}_2\text{Cu}_3\text{O}_{7-\delta}$ in the temperature range $377\text{--}812^\circ\text{C}$ from the oxygen ion conductivity,²⁶ measured by a complex impedance technique, using yttria-stabilized ZrO_2 (YSZ) electrodes that were blocking for the electron or hole current, but transparent for the oxygen ion current. Since the transference number for electrons in YSZ (Refs. 27) appears to be greater than that for oxygen ions in $\text{YBa}_2\text{Cu}_3\text{O}_{7-\delta}$, the ramifications of this measurement are not clear.

D. Comparison with theory

As mentioned in Sec. I, all of the theories of oxygen diffusion in $\text{YBa}_2\text{Cu}_3\text{O}_{7-\delta}$ are flawed. For example, Ronay and Nordlander³ considered neither the effect of increasing disorder of the oxygen with temperature, and the effect this would have on the open channels, nor the energy required to move an oxygen ion into an open channel. Tu *et al.*⁴ neglected correlation effects, and Bakker *et al.*⁵ calculated the activation energy by normalization to experimental data from chemical diffusion experiments. Each model thus has one or more unsatisfactory aspects.

The calculation of Ronay and Nordlander predicts activation barriers of 1.7 and 1.6 eV in the a and c directions, respectively, and 0 in the b direction. While the calculation is, admittedly, only valid for low temperatures, it is hard to reconcile with our value of 0.97 eV for the fast-diffusing component, which, according to their model, is for the b direction. Untwinned orthorhombic single crystals large enough to measure the anisotropy within the ab plane and thus test this theory are not yet available.

The model of Tu *et al.* predicts that the activation energy for oxygen vacancy diffusion is 1.3 eV for $\delta=0$ and ≈ 0.5 eV for $\delta=0.38$. This is not in accord with our result that D_1 may be described by a single activation energy over a wide range of stoichiometry; the data presented in Fig. 7 for $\text{P}_{\text{O}_2} = 10^5$ Pa cover a range of δ from 0.68 at 850°C to 0.12 at 300°C ,² and no obvious curvature in the Arrhenius plot is observed. Furthermore, the variation of D with oxygen pressure, covering a range of δ between 0.31 and 0.44, indicates that any change of D_1 with δ is less than a factor of 2 (Fig. 10).

Much of the temperature dependence of D in the theory of Bakker *et al.*⁵ is in the temperature dependence of the correlation factor. This increases strongly with increasing temperature at low temperatures because of the disordering of the vacancies; since the dependence of the correlation factor on the temperature is not expected to

be of the Arrhenius type, it is surprising that the diffusion coefficient obeys an Arrhenius relationship. Further, as the O - T transformation temperature is approached, the ordering of vacancies between the $O(1)$ and $O(5)$ sites no longer changes, so this term in the temperature dependence goes to zero, and the activation energy should decrease correspondingly, resulting in a downward curvature of the Arrhenius plot, which is not observed. This model also predicts a very mild decrease of D with increasing P_{O_2} for $T < T_{O-T}$, contrary to the observation in Fig. 10, although this is not viewed as a serious discrepancy because of the uncertainties in the data. We are reluctant to speculate on the value of D_0 , $1.4 \times 10^{-4} \text{ cm}^2 \text{ s}^{-1}$, which is lower than commonly found for vacancy diffusion in simple systems.

V. SUMMARY

Measurements of oxygen tracer diffusion in $\text{YBa}_2\text{Cu}_3\text{O}_{7-\delta}$ indicate that diffusion is highly anisotropic. Diffusion in the ab plane is much faster than diffusion along the c axis. The Arrhenius plot for diffusion in the ab plane extends across the orthorhombic-tetragonal

transformation temperature with an activation energy of $0.97 \pm 0.03 \text{ eV}$. The diffusion coefficient is not a sensitive function of P_{O_2} from $3 \times 10^3 \text{ Pa}$ to 10^5 Pa at 600°C . None of the proposed theories fit all of the features of the experimental data.

ACKNOWLEDGMENTS

The authors are grateful to K. C. Goretta, N. Chen, and J. P. Singh, who provided the samples. We are also pleased to acknowledge L. J. Thompson for computer programming, B. Tani for texture measurements, and L. J. Nowicki for experimental assistance. We are grateful to H. Bakker, D. O. Welch, J. L. Tallon, and K. N. Tu for sending us copies of their work, prior to publication, and to K. C. Goretta, K. Persels, and J. N. Mundy for valuable discussions. The SIMS analyses were carried out in the Center for Microanalysis of Materials, University of Illinois, which is supported by the U.S. Department of Energy under Contract No. DE-AC 02-76ER01198. This work was supported by the U.S. Department of Energy, BES-Materials Sciences, under Contract No. W31-109-ENG-38.

- ¹J. D. Jorgensen, H. Shaked, D. G. Hinks, B. Dabrowski, B. W. Veal, A. P. Paulikas, L. J. Nowicki, G. W. Crabtree, W. L. Kwok, L. H. Nunez, and H. Claus, *Physica C* **153-155**, 578 (1988).
- ²J. D. Jorgensen, M. A. Beno, D. G. Hinks, L. Soderholm, K. J. Volin, R. L. Hitterman, J. D. Grace, I. K. Schuller, C. U. Segre, K. Zhang, and M. S. Kleefisch, *Phys. Rev. B* **36**, 3608 (1987).
- ³M. Ronay and P. Nordlander, *Physica C* **153-155**, 834 (1988).
- ⁴K. N. Tu, N. C. Yeh, S. I. Park, and C. C. Tsuei, *Phys. Rev. B* **39**, 304 (1989).
- ⁵H. Bakker, J. P. A. Westerveld, D. M. R. Lo Cascio, and D. O. Welch, *Physica C* **157**, 25 (1989).
- ⁶J. L. Routbort, S. J. Rothman, L. J. Nowicki, and K. C. Goretta, *Mater. Sci. Forum* **34-36**, 315 (1988).
- ⁷J. L. Routbort and S. J. Rothman, *Acta Ceramica* (to be published).
- ⁸S. J. Rothman, J. L. Routbort, J. E. Baker, L. J. Nowicki, K. C. Goretta, L. J. Thompson, and J. N. Mundy, in *Diffusion Analysis and Applications*, edited by A. D. Romig, Jr. and M. A. Dayananda (The Minerals, Metals, and Materials Society, Warrendale, Pennsylvania, 1989), p. 289.
- ⁹S. J. Rothman and J. L. Routbort, in *Diffusion and Materials*, NATO Advanced Study Institute, Series E: Engineering and Materials Science, edited by G. Brebec, A. L. Laskar, and C. Monty [Kluwer Academic, Dordrecht (in press)].
- ¹⁰D. S. Tannhauser, J. A. Kilner, and B. C. H. Steele, *Nucl. Instrum Methods* **218**, 504 (1983).
- ¹¹C. Dubois, C. Monty, and J. Philibert, *Philos. Mag. A* **46**, 419 (1982).
- ¹²S. Yamaguchi and M. Someno, *Trans Jpn. Inst. Met.* **23**, 259 (1982).
- ¹³J. L. Routbort and S. J. Rothman, *J. Phys. Chem. Solids* **47**, 993 (1986).
- ¹⁴J. L. Routbort, S. J. Rothman, B. K. Flandermeyer, L. J. Nowicki, and J. E. Baker, *J. Mater. Res.* **3**, 116 (1988).
- ¹⁵*SAS User's Guide: Statistics* (SAS Institute, Cary, North Carolina, 1985) pp. 575-607.
- ¹⁶J. F. Nye, *The Physical Properties of Crystals* (Oxford University Press, Oxford, 1975), p. 195.
- ¹⁷S. J. Rothman, J. L. Routbort, L. J. Nowicki, J. E. Baker, D. M. Ginsberg, P. D. Han, D. A. Payne, and J. P. Rice (unpublished).
- ¹⁸D. G. Hinks, B. Dabrowski, K. Zhang, C. U. Segre, J. D. Jorgensen, L. Soderholm, and M. A. Beno, in *High-Temperature Superconductors*, Vol. 99 of *Materials Research Society Symposium Proceedings Series, Boston, 1988*, edited by M. B. Brodsky (Mass. Mater. Res. Soc., 1988), p. 9.
- ¹⁹Nan Chen, MS thesis, Illinois Institute of Technology, 1989.
- ²⁰Y. Ikuma and S. Akiyoshi, *J. Appl. Phys.* **64**, 3915 (1988).
- ²¹J. L. Tallon and M. P. Staines (private communication).
- ²²H. Bakker, J. P. A. Westerveld, and D. O. Welch, *Physica* **147B**, 161 (1987).
- ²³Note that this is not the interdiffusion coefficient obtained in, say, an A/B metallic diffusion couple.
- ²⁴It seems likely the f_v and f are quite close in value since the ordering has the same effect on the atom and vacancy jumps.
- ²⁵See, e.g., L. Heyne in *Solid Electrolytes*, edited by S. Geller (Springer, Berlin, 1977), p. 193.
- ²⁶D. J. Vischjager, P. J. Van Der Put, J. Schram, and J. Schoonman, *Solid State Ionics* **27**, 199 (1988).
- ²⁷L. Heyne and N. M. Beekmans, *Proc. Br. Ceram. Soc.* **19**, 229 (1971).

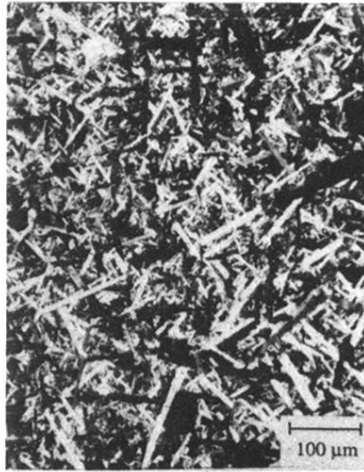


FIG. 2. Micrograph of $\text{YBa}_2\text{Cu}_3\text{O}_{7-\delta}$ made from material No. 1 taken using polarized light. The bar represents $100\ \mu\text{m}$.